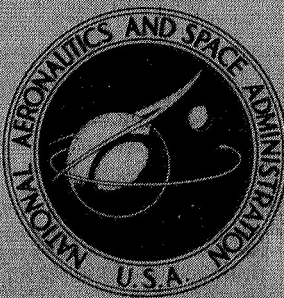


NASA TECHNICAL
MEMORANDUM



NASA TM X-1641

NASA TM X-1641

N 68-32988

(ACCESSION NUMBER)	(PAGES)	(THRU)
25	1	
TMX-1641		(CODE)
		33
(NASA CR OR TMX OR AD NUMBER)		
(CATEGORY)		

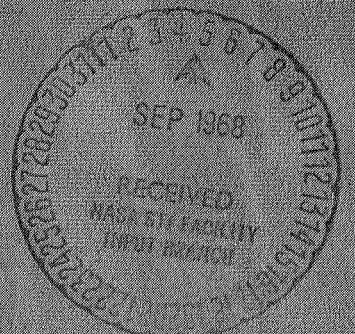
GPO PRICE \$ _____
CFSTI PRICE(S) \$ _____
Hard copy (HC) _____
Microfiche (MF) _____

ff 653 July 65

COMPARISON OF EXPERIMENTAL
AND PREDICTED HEAT TRANSFER
CHARACTERISTICS FOR A
CYLINDRICAL EJECTOR

by Francis C. Chenoweth and Fred W. Steffen

Lewis Research Center
Cleveland, Ohio



NATIONAL AERONAUTICS AND SPACE ADMINISTRATION • WASHINGTON, D. C. • AUGUST 1968

NASA TM X-1641

**COMPARISON OF EXPERIMENTAL AND PREDICTED HEAT TRANSFER
CHARACTERISTICS FOR A CYLINDRICAL EJECTOR**

By Francis C. Chenoweth and Fred W. Steffen

Lewis Research Center
Cleveland, Ohio

NATIONAL AERONAUTICS AND SPACE ADMINISTRATION

For sale by the Clearinghouse for Federal Scientific and Technical Information
Springfield, Virginia 22151 - CFSTI price \$3.00

ABSTRACT

The heat transfer characteristics of a cylindrical ejector for a small afterburning turbojet engine operating at static sea level conditions were compared with film-cooling correlations based on an insulated wall. Since the ejector in this test was not insulated, a correction for radiation and free-convection losses was derived and applied to the wall temperatures calculated using one of the correlations. Good agreement was obtained between the experimental and predicted wall temperatures.

COMPARISON OF EXPERIMENTAL AND PREDICTED HEAT TRANSFER CHARACTERISTICS FOR A CYLINDRICAL EJECTOR

by Francis C. Chenoweth and Fred W. Steffen

Lewis Research Center

SUMMARY

The heat transfer characteristics of a cylindrical ejector for a small afterburning turbojet engine operating at static sea level conditions were compared with three film-cooling correlations based on an insulated wall. Since the ejector in this test was not insulated, a correction for radiation and free convection was derived and applied to the wall temperatures calculated using one of the correlations.

The Hatch-papell correlation predicted wall temperatures which were low near the coolant slot and extremely high near the end of the cylindrical shroud. The Goldstein, Eckert, et al., correlation was optimistic in predicting wall temperatures equal to the coolant temperature. The wall temperatures predicting wall temperatures equal to the coolant temperature. The wall temperatures predicted using the Lucas-Golladay correlation agreed well for wall temperatures less than 1300° R (722 K) but diverged to an error of 600° R (333 K) near the ejector exit. However, upon applying the wall temperature correction for radiation and free-convection effects, the predicted data agreed with the experimental data to within 150° R (83.2 K).

INTRODUCTION

Many current aircraft jet propulsion systems make use of an ejector to provide cooling airflow over the engine tailpipe. At static or takeoff conditions, the total pressure of the coolant is generally equal to or less than the ambient static pressure so that energy must be transferred from the primary jet to the coolant flow to accomplish the pumping. The coolant flow is used to cool the ejector shroud by providing an insulating layer of cool air between the hot gas jet and the shroud. This cooling method is called "film cooling." Several experimental investigations have been made of the

film cooling of an insulated wall; however, the shroud of an ejector is not insulated.

The purpose of this investigation was to measure the heat-transfer characteristics of a cylindrical ejector under simulated engine operating conditions and to determine if any existing film-cooling correlation schemes can be used to predict the shroud material temperatures.

The tests were conducted in a sea-level static test facility using a J85/13 after-burning turbojet as the primary gas generator. Two engine power settings were run providing hot gas stream stagnation temperatures of about 3540° R (1965 K) and 3000° R (1665 K). The coolant stagnation temperature was about 520° R (289 K) for each setting. The hot gas stream was made up of JP-4 and air combustion products, at a stagnation pressure of about 30 psia (21 N/cm^2). The hot gas stream Mach number varied from about 1.0 to 1.36. Air was used as the coolant; the coolant Mach number varied from 0.28 to 0.60.

SYMBOLS

A	area
C	constant
C_p	specific heat
D	diameter
erf	error function
F	configuration factor for radiant energy exchange
f()	function of
Gr	Grashof number
h	heat transfer coefficient
k	thermal conductivity
K'	constant from references 3 and 4
L	length
P	total pressure
p	static pressure
Pr	Prandtl number
q	heat flux

Re Reynolds number
S slot width, shroud radius minus primary radius for cylindrical ejector
T total temperature of fluid or metal temperature
t static temperature
V velocity
w weight flow rate
x axial distance downstream of cooling slot
y radial distance from boundary of the jet
 α^* thermal diffusivity
 β_{eff} effective coolant injection angle, ref. 4
 ϵ emissivity
 η_r cooling efficiency with recovery temperature of hot gas stream acting as the driving temperature
 η_s cooling efficiency with static temperature of hot gas stream acting as the driving temperature
 ρ density
 σ Stefan-Boltzmann constant

Subscripts:

c carbon dioxide
D based on diameter
f film, arithmetic mean of secondary and primary temperatures
gr gray
i denotes surface of higher temperature
j denotes surface of lower temperature
p primary
r recovery
S shroud
s secondary
w wall
wa water
 ∞ ambient

APPARATUS AND PROCEDURE

Apparatus

The tests were conducted in a static test facility at atmospheric pressure and temperature. A turbojet engine (J-85/13) with an afterburner and variable area primary nozzle was used as the primary gas generator.

Figure 1 is a sketch of the ejector shroud and primary nozzle. A single fixed-geometry shroud was used during the investigation. The shroud was fabricated from 0.050-inch (0.127 cm) thick Inconel 600. It was attached directly to the engine variable exhaust nozzle housing. Wall static pressure taps and wall temperature thermocouples were installed on the cylindrical shroud. Their locations are also shown in figure 1. Figure 2 shows the cylindrical ejector installed in the test facility.

Procedure

The data were obtained at two engine power settings. These power settings were maximum reheat and reheat A (the power setting just below maximum reheat for this particular engine). For each power setting, the primary nozzle area was set by the engine control system to a value which maintained a constant turbine exit temperature. In this manner, two shroud diameter to primary nozzle diameter ratios were obtained. Also, the design of the primary nozzle was such that as the primary nozzle diameter increased, the exit plane of the primary nozzle moved upstream, thereby minimizing changes in shroud-length to primary-nozzle-diameter ratios. The shroud-diameter to primary-nozzle-diameter ratios and the corresponding ejector-length to primary-nozzle-diameter ratios are contained in table I. Although engine fuel flow and airflow were measured during the test, the primary gas pressure, primary temperature and primary nozzle area were not measured but were assumed to be equal to the published values of reference 1 for the engine used as the primary gas generator. The primary temperature used for the film-cooling calculations was 5 percent greater than the average hot-gas total temperature. This increase accounts for the radial temperature distortion profile of this particular afterburner design which produces maximum temperatures near the wall. These values are also contained in table I.

The secondary weight flow rate was calculated with the aid of the flow model shown in figure 3 and the ejector static pressure distributions from figure 4. These pressures are plotted as a function of the distance from the primary nozzle exit plane in the maximum afterburning position. The calculation was made using the conditions at a station coincident with the most upstream static pressure tap. It was assumed that the static pressure of the secondary and primary flow were uniform at this station and equal

to the measured wall static pressure. It was also assumed that the total pressure and total temperature of the secondary flow at this station were ambient and that no energy exchange between streams had occurred upstream of this station. Using this published value of the primary total pressure with the measured wall static pressure and assuming a one-dimensional expansion, the flow area occupied by the primary jet and the flow area remaining for the secondary stream were determined. Then, using the secondary flow area, total and static pressure, and total temperature, a secondary weight flow was calculated. These calculated secondary weight flow rates are included in table I. The initial Mach number of the coolant stream was calculated based on the ratio of ambient pressure to the static pressure at the most upstream static pressure tap. This is the same station at which secondary weight flow was calculated.

ANALYSIS PROCEDURE

Discussion of Film-Cooling Correlations

Film-cooling of surfaces using gases has been the subject of many investigations. Some excellent discussions of the correlations for film-cooling are available in the literature (refs. 2 to 7). In each case, the discussion leads to a recommended correlation. The geometrical configuration of a cylindrical ejector is different from any of the configurations studied in these previous investigations, however.

An experimental investigation was made by Papell and Trout (ref. 2) for the film-cooling apparatus shown in figure 5(a). The adiabatic surface, which is to be protected from the hot gas flowing over it, is interrupted by a step-down slot from which the coolant is injected in the downstream direction. Hatch and Papell (ref. 4) then correlated the data obtaining the following equation

$$\ln \eta_r = \ln \left(\frac{T_r - T_w}{T_r - t_s} \right) = - \left(\frac{\pi D x h_f}{W_s C_{p,s}} - K' \right) \left(\frac{S V_p}{\alpha_s} \right)^{0.125} f \left(\frac{V_p}{V_s} \right) + \ln \cos 0.8 \beta_{eff} \quad (1)$$

where

$$h_f = 0.0265 \frac{k_f}{D} Re_f^{0.8} Pr_f^{0.3} \quad (2)$$

and

$$f \left(\frac{V_p}{V_s} \right) = 1 + 0.4 \tan^{-1} \left[\left(\frac{V_p}{V_s} \right) - 1 \right] \quad \text{for } \frac{V_p}{V_s} \geq 1.0$$

or

$$f\left(\frac{V_p}{V_s}\right) = \left(\frac{V_s}{V_p}\right)^{1.5} \left[(V_s/V_p) - 1 \right] \quad \text{for } \frac{V_p}{V_s} < 1.0$$

For the experimental conditions of reference 2, the value of K' was 0.04.

Lucas and Golladay in applying equation (1) to an insulated rocket nozzle (fig. 5(b)) (refs. 5 and 6), proposed the following changes:

- (1) The constant K' from 0.04 to 0.0
- (2) The use of local hot gas static temperature as the driving temperature rather than the recovery temperature
- (3) The use of an integrated average of heat transfer coefficient from the coolant injection station to the separate data stations.

The first two of these changes were used in processing the data for this report; however, the heat transfer coefficient defined by equation (2) was used. For the cylindrical ejector tested, the coolant velocity is very nearly constant from the coolant injection station (primary nozzle exit plane) to the ejector exit; therefore, the change in heat transfer coefficient along its length is assumed to be negligible. With these changes incorporated, equation (1) becomes

$$\ln \eta_s = \ln \left(\frac{t_p - T_w}{t_p - t_s} \right) = - \left(\frac{\pi D h_f}{w_s C_{p,s}} \right) \left(\frac{S V_p}{\alpha_s} \right)^{0.125} f\left(\frac{V_p}{V_s}\right) + \ln \cos 0.8 \beta_{eff} \quad (3)$$

An experimental study of film cooling in high-speed flow was made by Goldstein, Eckert, Tsou and Haji-Sheikh (ref. 7) with a configuration such as that shown in figure 5(c). The coolant is injected parallel to the hot stream as in figure 5(a); however, the hot stream is supersonic. Goldstein, Eckert, et al., recommend (ref. 7) the efficiency be obtained from

$$\eta_r = \frac{T_r - T_w}{T_r - T_s} = 162.0 \left[\frac{(\rho V)_s S}{(\rho V)_p x} \right]^{1.2} \quad (4)$$

for

$$\frac{(\rho V)_s}{(\rho V)_p} > 0.12$$

This equation is based on data for secondary flow temperatures higher than the primary flow temperature (film-heating).

The range of experimental conditions used to formulate the three correlations is shown in table II. The range of test conditions applied to the cylindrical ejector is also shown. Many differences and similarities existed. The correlations from references 2, 3, 4, and 7 were derived for a flat plate. Lucas and Golladay tested a convergent-divergent nozzle and modified the Hatch-Papell correlation. The flows considered in references 5 to 7 and in the present cylindrical ejector were supersonic. The flow was also accelerating in references 5 and 6. The flow acceleration in the cylindrical ejector was relatively minor, however, and was neglected. The hot-stream Mach number of the cylindrical ejector, 1.0-1.36, was within the range of the Lucas-Golladay tests (0.5-3.0). The stagnation temperature of the cylindrical ejector ranged from 3000° F (1665 K) to 3540° R (1965 K). The maximum temperature obtained in reference 7 was 530° R (294 K). Hatch and Papell (refs. 2 to 4) and Goldstein, Eckert, et al., (ref. 7) used both air and helium as coolants. Lucas and Golladay (refs. 5 and 6) used nitrogen. As has been stated previously, the cylindrical ejector pumped air to cool the shroud.

Discussion of Wall Temperature Correction

The external surfaces of the three configurations for which correlations were developed were insulated. The cylindrical ejector was not insulated; and, therefore, there was heat transfer by radiation and free convection from the surface to the surroundings.

A wall temperature correction method was developed for, and was applied to, the Lucas-Golladay correlation. It was not applied to the Hatch-Papell correlation because of the similarity to the Lucas-Golladay correlation. The Goldstein, Eckert, et al., correlation was not corrected because there was not sufficient information available about the experimental apparatus to develop the correction.

To correct the predicted wall temperatures obtained using an insulated convergent-divergent nozzle correlation to wall temperatures for a noninsulated cylindrical ejector, the following assumptions were made:

- (1) There was no temperature gradient through the wall
- (2) The forced convection heat transfer coefficient between the wall and the coolant would be the same for an insulated wall and a noninsulated wall (i.e., it would not vary with wall temperature)
- (3) The axial heat transfer rate in the wall was negligible
- (4) The mixing of the hot gas stream and the coolant stream would be the same for an insulated wall and a noninsulated wall.

A heat balance on the wall element shown in figure 6 follows for the "noninsulated" case:

$$q_1 - q_2 - q_3 - q_4 - q_5 = 0 \quad (5)$$

where the subscripts are defined as

- 1 hot gas to wall radiation
- 2 wall to coolant forced convection
- 3 inside wall to ambient radiation
- 4 outside wall to ambient radiation
- 5 outside wall to ambient free convection

The subscripts apply to figure 6 also. For the "insulated case"

$$q_4 = q_5 = 0$$

Equation (5) then becomes:

$$q_1 - q_2 - q_3 = 0 \quad (6)$$

Writing equations (5) and (6) in terms of heat transfer coefficients and temperature differences, assuming all heat transfer areas are equal, results in

$$h_1(t_p - T_w) - h_2(T_w - t_s) - h_3(T_w - t_\infty) - h_4(T_w - t_\infty) - h_5(T_w - t_\infty) = 0 \quad (7)$$

and

$$h'_1(t_p - T'_w) - h'_2(T'_w - t_s) - h'_3(T'_w - t_\infty) = 0 \quad (8)$$

where the prime signifies the insulated case. The radiation heat transfer coefficients h_1 , h_3 and h_4 were obtained from

$$q = F_{ij} \sigma(T_i^4 - T_j^4) = h(T_i - T_j)$$

Therefore, h was defined as

$$h = \frac{F_{ij} \sigma(T_i^4 - T_j^4)}{(T_i - T_j)}$$

The configuration factors F_{ij} will be discussed later. The average free-convection coefficient for a horizontal cylinder is (ref. 8):

$$h_5 = 0.53 \frac{k}{D} (Gr_D Pr)^{1/4}$$

This equation is valid for the Prandtl numbers greater than 0.5 and Grashof numbers ranging from 10^3 to 10^9 . Properties are obtained at the arithmetic mean between the wall temperature and ambient temperature.

Solving for the convective heat transfer coefficient between the wall and the coolant for both cases, from equations (7) and (8)

$$h_2 = \frac{(h_3 + h_4 + h_5)(T_w - t_\infty) - h_1(t_p - T_w)}{t_s - T_w} \quad (9)$$

and

$$h'_2 = \frac{h'_3(T'_w - t_\infty) - h'_1(t_p - T'_w)}{(t_s - T'_w)} \quad (10)$$

Then applying assumption 2

$$h_2 = h'_2$$

or, equating (9) and (10)

$$\frac{(h_3 + h_4 + h_5)(T_w - t_\infty) - h_1(t_p - T_w)}{t_s - T_w} = \frac{h'_3(T'_w - t_\infty) - h'_1(t_p - T'_w)}{t_s - T'_w} \quad (11)$$

Equation (11) was then solved for the noninsulated wall temperature T_w

$$T_w = \frac{\frac{h'_3(T'_w - t_\infty) - h'_1(t_p - T'_w)}{t_s - T'_w} t_s + (h_3 + h_4 + h_5)t_\infty + h_1 t_p}{h_1 + h_3 + h_4 + h_5 + \frac{h'_3(T'_w - t_\infty) - h'_1(t_p - T'_w)}{t_s - T'_w}} \quad (12)$$

Since h_1 , h_3 , h_4 and h_5 were a function of the wall temperature, an iteration was required for the solution of the corrected wall.

The right-hand side of equation (10) was calculated based on the wall temperature obtained using the Lucas-Golladay correlation. This is then a constant for the iteration at a particular station, with no change in flow conditions. For the first approximation, the other heat transfer coefficients in equation (12) were also based on this wall temperature. A new wall temperature was calculated from equation (12). Then h_1 , h_3 ,

h_4 and h_5 were recalculated based on this new wall temperature. This iteration was continued until the estimated temperature was equal to the calculated temperature within some predetermined tolerance.

The configuration factors used were obtained as follows. The configuration factor for the radiant energy exchange between the hot gas and the wall was estimated according to the procedure presented in reference 9. Since the hot gas was made up of the combustion products of air and JP-4, the nonluminous radiation of the carbon dioxide and water vapor had to be considered. The luminous radiation is neglected since very little free carbon is present. It was reported in reference 10 that the assumption of nonluminous radiation adequately accounted for all the radiant heat load. The nonluminous radiation was calculated as presented by Weibelt in reference 9:

$$\epsilon_p = \epsilon_c C_c + \epsilon_{wa} C_{wa} + \Delta\epsilon$$

where

ϵ_p	emittance of the hot gas
ϵ_c	emittance of CO_2
C_c	correction for total pressure and partial pressure for CO_2
ϵ_{wa}	emittance of H_2O
C_{wa}	correction for total pressure and partial pressure for H_2O
$\Delta\epsilon$	correction for a mixture of CO_2 and H_2O

This work was first presented in reference 11 by H. C. Hottel.

A nondimensional comparison of the convergent-divergent nozzle used for the Lucas-Golladay correlation (ref. 6) and the cylindrical ejector of this study is made in figure 7. The reference diameter, D , was the minimum of the film-cooled surface diameters for both cases. These were the throat diameter for the C-D nozzle and the shroud inside diameter for the cylindrical ejector. The length, x , was the axial length from the coolant injection slot.

The configuration factors for the radiation heat transfer from the inside surface to the ambient are also shown in figure 7. The values for the noninsulated cylinder were obtained from reference 12. Reference 13 was the source of the values for the convergent-divergent nozzle. A surface emissivity of 0.9 was used for both configurations.

Values from the dotted line were used to obtain the inside radiation heat transfer coefficient for the insulated configuration (h'_3). The heat transfer coefficient for the inside radiation of the noninsulated configuration (h_3) was taken from the solid line.

For a point of calculation, the values were chosen at equal values of x/D . For the C-D nozzle at values of x/D less than 0.4, the configuration factor was assumed to be zero since these surfaces are upstream of the throat and essentially do not radiate to the ambient.

In figure 7, the overall length-to-diameter ratio for the C-D nozzle is larger than that of the cylindrical ejector by a factor of approximately 2. Because of this, the configuration factors near the end of the cylindrical ejector are considerably larger than those at an equal value of x/D for the C-D nozzle. For x/D between 0.0 and 1.25, the configuration factors for both cases are almost equal.

The configuration factor for the outside surface radiation to the ambient was obtained as follows: for gray bodies, the radiative interchange factor for an enclosed body and its enclosure is given in reference 14 as

$$(F_{ij})_{gr} = \frac{\epsilon_i}{1 + \epsilon_i \left(\frac{1}{\epsilon_j} - 1 \right) \frac{A_i}{A_j}} \quad (13)$$

where the subscripts i and j refer to the inner body and the enclosure. For the case considered here

$$A_j \gg A_i$$

therefore, equation (13) reduces to

$$(F_{ij})_{gr} = \epsilon_i$$

The constant value of 0.9 was assumed over the entire length of the ejector shroud.

The coolant temperature t_s used in the Lucas-Golladay correlation, was the inlet temperature. However, when applying the coolant temperature in the wall temperature correction procedure, it was necessary that the coolant temperature be known as a function of length. This axial temperature distribution of the coolant was obtained using the analytical procedure developed in reference 15. In applying this isoenergetic mixing theory to the cylindrical ejector, the following assumptions were made. The total-temperature spreading rate during the mixing process was the same as that of the momentum. Therefore, the total-temperature profile was the same as the velocity profile. The secondary stream Mach number was assumed to be zero. With these assumptions, the temperature distribution is then expressed as:

$$\frac{T(x, y) - T_s}{T_p - T_s} = \frac{1}{2} \left[1 + \operatorname{erf} \left(12 \frac{y}{x} \right) \right]$$

This temperature distribution was assumed the same for the insulated and noninsulated cases.

RESULTS AND DISCUSSION

Experimental and predicted (but uncorrected) wall temperatures are compared in figure 8. The reference point used for comparison is the axial location of the primary nozzle exit plane in the maximum reheat position. When the engine is operating at the reheat A condition, the exit plane is downstream approximately 0.5 inch (1.27 cm).

The average hot-gas total temperature was obtained from reference 1 as a function of the fuel-to-air ratio. The fuel-to-air ratio was measured. The primary temperature used to predict wall temperatures was 5 percent greater than the average hot-gas temperature. This increase accounts for the radial temperature distortion profile of this particular afterburner design which produces maximum temperatures near the wall.

Since the fuel-to-air ratio varied for repeat points at each engine condition, the primary temperatures varied also. For the maximum reheat engine setting (fig. 8(a)), the total temperature of the primary stream varied 52° R (29 K). This variation gave a variation in predicted wall temperatures of less than 10° R (5.6 K). For the reheat A engine setting (fig. 8(b)), the total temperature varied 41° R (22.8 K) which caused a vibration of 10° R (5.6 K) in predicted wall temperatures. Therefore, the scatter in primary temperature had only a minor effect on the predicted results.

The maximum spread in experimental wall temperature was $\pm 100^{\circ}$ R (± 55.5 K) for the maximum reheat engine setting and $\pm 125^{\circ}$ R (± 69.4 K) for the reheat A conditions.

The cylindrical ejector extends into the test facility exhaust duct two inches (5.08 cm). This can be seen in figure 2. The pumping action created by the high velocity of the exhaust gas causes air from the test cell to flow over the last few inches of the cylindrical ejector. Convective heat transfer to this airflow caused the wall temperature to be lower near the end of the ejector. An attempt to correct the wall temperature was not made since it is a facility effect.

As the system was cycled from ambient temperature to 3500° R (1945 K), several thermocouples broke loose from the surface. This accounts for the decreased number of points at several locations along the shroud.

The predicted wall temperatures presented in figure 8 were not corrected for radiation and nonadiabatic wall heat losses. For the maximum reheat case (fig. 8(a)), the Lucas-Golladay prediction agrees reasonably well with experimental data near the nozzle. Downstream from the nozzle the measured temperatures are much lower than

the predicted temperatures. At the point where the jet pumping of air along the outer side of the cylindrical ejector is seen to affect the wall temperature (about 22 inches (55.9 cm)), the difference between predicted and measured wall temperature is about 600° R (333 K). This error is believed to be due to radiation and free-convection losses from the shroud's external surface which were not considered in the correlation. The difference between measured wall temperature and ambient temperature is seen to vary from about 500° R (278 K) at the station closest to the nozzle to about 1300° R (722 K) at x equal to 22 inches (55.9 cm).

For the reheat A condition (fig. 8(a)), the Lucas-Golladay predicted wall temperatures agree very well with the measured temperatures, up to the 22-inch (55.9 cm) station. The wall temperatures are much lower for this case, however. The maximum difference from wall to ambient for this case is seen to be about 900° R (500 K). Thus, radiation and free-convection heat losses will be much lower for the reheat A condition than for the maximum reheat condition.

The wall temperatures predicted using the Hatch-Papell correlation, equation (1), predict low temperatures near the point of coolant injection and high temperatures near the end of the cylindrical ejector. The predictions are approximately 500° R (-278 K) low near the primary nozzle and about 900° R (500 K) high at 22 inches (55.9 cm) from the point of coolant injection.

The constant wall temperature for the first 4 inches (10.16 cm) in the maximum-reheat condition, and the first 12 inches (30.5 cm) of the reheat A condition indicates the predicted distance the coolant flows along the wall before its temperature increases. The experimental data indicate a rise in wall temperature immediately downstream of the primary nozzle.

Radiation heat transfer from the hot-gas stream to the wall obviously caused an increase in wall temperature, although the coolant is at a lower temperature than either the wall or the hot stream. The coolant (air) would not be heated appreciably by this radiation heat transfer. Thus, the coolant was being heated by the wall as well as being mixed with the hot gas for the first few inches. Further downstream, the coolant stream temperature was hotter than the wall and heat was transferred from the "coolant" to the wall.

The predicted wall temperatures obtained using the Goldstein, Eckert, et al., correlation, equation (4), was a constant equal to the static temperature of the coolant (490° R (272 K)). The reason for this optimistic prediction of wall temperature is believed to be due, at least in part, to the absence of radiant energy exchange (hot stream to wall) in the experiment for which the correlation was derived. This also illustrates the danger of trying to use an empirical correlation at conditions far removed from the conditions at which the correlation was developed.

As stated previously, the wall temperatures predicted using the Lucas-Golladay

correlation were corrected using equation (12). The results are compared with the uncorrected predictions and experimental data in figure 9. The uncorrected predicted data and the experimental data are the same as shown in figure 8. As expected, the higher the wall temperature (assuming a constant ambient temperature), the larger the effect of the radiation and free-convection corrections. Generally speaking, the correction required for wall temperatures below 1200° R (666 K) is less than 100° R (55 K).

Upon applying the heat loss correction to the maximum reheat engine condition (fig. 9(a)), the predicted wall temperatures agree within 150° R (83.4 K) with those obtained experimentally. The maximum correction, with the exception of those points downstream of 22 inches (55.9 cm) was 600° R (333 K). The correction equation applied to the reheat A data (fig. 9(b)), yielded a slight overcorrection, however. The uncorrected predictions were reasonably good. The corrected temperatures tended to be slightly low, especially on the hot end of the ejector.

A comparison is made of the relative heat transfer rates between the hot gas and the wall and between the wall and the ambient in figure 10. The heat transferred to the wall by radiation is higher near the point of coolant injection and decreases toward the ejector exit. This decrease is due to the decrease in the difference of the hot gas and wall temperature.

The net heat transfer from the wall to the coolant is the difference of the hot gas to wall radiation and the sum of the three heat losses shown in figure 10. As previously discussed, the heat flow near the point of coolant injection is from the wall to the coolant. At approximately 22 inches (55.8 cm) this direction changes and the heat flows from the coolant to the wall.

At a distance of 4 inches (10.16 cm) from the point of coolant injection, the free-convection loss is approximately 4 percent of the total heat loss from the wall. The radiation from the outer wall is approximately 8 percent. The radiation loss from the inside is negligible. The loss of heat to the coolant then is about 88 percent of the total loss. At 18 inches (45.7 cm) the radiation loss from the inside and the free convection from the outside make up a total of approximately 16 percent of the total loss. The percent of heat loss by radiation from the outside has increased to approximately 70 percent. Therefore, the heat transfer from the wall to the coolant is only 14 percent of the total loss. At the ejector exit, the three losses shown on figure 10 add up to produce 120 percent of the heat added by radiation from the hot gas to the wall. Therefore, the heat added to the wall from the coolant is about 20 percent of that added by radiation from the hot gas stream.

It is believed this wall temperature correction could be applied to the other correlations presented if enough were known of the geometry used to obtain the correlations. In applying this correction for design purposes, it would be necessary to obtain a heat

balance for the new noninsulated hardware. Therefore, an equation similar to equation (7) must be derived. For applying to a new correlation, an equation similar to equation (8) must also be obtained. Upon combining these two equations, an equation for the corrected wall temperature would be obtained for the new hardware. This equation would then be solved in the same manner as stated in this report.

CONCLUDING REMARKS

The heat transfer characteristics of a cylindrical ejector for a small afterburning turbojet engine operating at static sea level conditions were compared with results using three film-cooling correlations available in the literature. The three semi-empirical correlations were each derived for geometries and flow conditions considerably different than those described in this report and utilized an insulated wall. The following results were obtained:

1. The prediction of wall temperature by the three correlations were in poor agreement with each other due to the varied conditions for which the correlations were derived.
2. The Hatch-Papell correlation, equation (1), uncorrected for radiation heat losses and nonadiabatic wall heat losses, predicted temperatures lower than experimental temperatures near the point of coolant flow injection and high temperatures near the end of the cylindrical shroud.
3. The Lucas-Golladay correlation, equation (3), predicted wall temperatures for the reheat A condition in which wall temperatures were less than 1500° R (832 K). For the maximum reheat case (maximum T_w 1900° R (1055 K)), the predicted wall temperatures exceed the measured values by as much as 600° R (333 K).
4. Upon applying a wall temperature correction, developed in this report, to the wall temperatures calculated using the Lucas-Golladay correlation, good agreement was obtained between the experimental and predicted data. This correction accounted for the convective and radiant heat losses from the noninsulated ejector wall.
5. The uncorrected Goldstein, Eckert, et al., correlation, equation (4), predicted wall temperatures equal to the coolant temperature. The measured wall temperatures varied from 750° R (416 K) to 1900° R (1055 K).

In applying this wall temperature correction for purposes of design, it should be

remembered that a new heat balance should be made for the hardware under consideration.

Lewis Research Center,

National Aeronautics and Space Administration,

Cleveland, Ohio, May 24, 1968,

126-15-02-10-22.

REFERENCES

1. Staff of General Electric: Model Specifications E1075, Engine, Aircraft, Turbojet, J85-GE-13. General Electric Co., Small Aircraft Engine Dept., June 1963.
2. Papell, S. Stephen; and Trout, Arthur M.: Experimental Investigation of Air Film Cooling Applied to an Adiabatic Wall by Means of an Axially Discharging Slot. NASA TN D-9, 1959.
3. Hatch, James E.; and Papell, S. Stephen: Use of a Theoretical Flow Model to Correlate Data for Film Cooling or Heating an Adiabatic Wall by Tangential Injection of Gases of Different Fluid Properties. NASA TN D-130, 1959.
4. Papell, S. Stephen: Effect on Gaseous Film Cooling of Coolant Injection Through Angled Slots and Normal Holes. NASA TN D-299, 1960.
5. Lucas, James G.; and Golladay, Richard L.: An Experimental Investigation of Gaseous-Film Cooling of a Rocket Motor. NASA TN D-1988, 1963.
6. Lucas, James G.; and Golladay, Richard L.: Gaseous-Film Cooling of a Rocket Motor with Injection Near the Throat. NASA TN D-3836, 1967.
7. Goldstein, R. J.; Eckert, E. R. G.; Tsou, F. K.; and Haju-Sheikh, A.: Film Cooling with Air and Helium Injection Through a Rearward-Facing Slot into a Supersonic Air Flow. HTL TR No. 60, University of Minnesota, Feb. 1965.
8. Kreith, Frank: Principles of Heat Transfer. Second ed., International Textbook Co., 1965.
9. Wiebelt, John A.: Engineering Radiation Heat Transfer. Holt, Rinehard & Winston, Inc., 1966.
10. Shillito, Thomas B.; and Smolak, George R.: Effect of Pressure Level on Afterburner-Wall Temperatures. NACA RM E58D01, 1958.

11. McAdams, William H.: Heat Transmission. Third ed., McGraw-Hill Book Co., Inc., 1954.
12. Sparrow, E. M.; Albers, L. U.; and Eckert, E. R. G.: Thermal Radiation Characteristics of Cylindrical Enclosures. J. Heat Transfer, vol. 84, no. 1, 1962, pp. 73-81.
13. Sparrow, E. M.; and Jonsson, V. K.: Radiant Emission Characteristics of Diffuse Conical Cavities. J. Opt. Soc., vol. 53, no. 7, July 1963, pp. 816-821.
14. Jakob, Max: Heat Transfer. Vol. 2, John Wiley & Sons, Inc., 1957.
15. Beheim, Milton A.; Klann, John L.; and Yeager, Richard A.: Jet Effects on Annular Base Pressure and Temperature in a Supersonic Stream. NASA TR R-125, 1962.

TABLE I. - EJECTOR GEOMETRIES AND FLOW CONDITIONS

Power setting	Ratio of secondary to primary diameter, D_s/D_p	Ratio of length to primary diameter, L/D_p	Primary area, A_p		Primary total pressure, P_p	
			in. ²	cm ²	psia	(N/cm ²)(abs)
Maximum reheat	1.10	1.88	174.3	1124.5	30.0	20.7
Reheat A	1.18	1.98	151.7	978.7	31.0	21.4

Power setting	Primary temperature		Primary weight flow rate, W_p		Secondary weight flow rate, W_s		Secondary temperature, T_s	
	$^{\circ}\text{R}$	K	lb/sec	kg/sec	lb/sec	kg/sec	$^{\circ}\text{R}$	K
Maximum reheat	3540	1966	44	19.95	5.7	2.59	520	289
Reheat A	3000	1667	44	19.95	11.3	5.13	520	289

TABLE II. - TABLE OF TEST CONDITIONS

	Hatch, Papell	Lucas, Golladay	Goldstein, Eckert, et al.	Cylindrical ejector	
				Maximum reheat	Reheat A
Reference	2, 3, 4	5, 6	7	-----	-----
Surface to be cooled	Flat plate	Convergent-divergent nozzle	Flat plate	Cylinder	Cylinder
Slot width, in. (cm)	0.063 (0.160) 0.050 (0.127)	0.04 (0.102), 0.045 (0.104)	0.064 (0.163) 0.123 (0.312) 0.182 (0.462)	0.75 (1.91)	1.25 (3.18)
Hot stream Mach number	0.15 to 0.70	0.5 to 3.0	3.01	1.0 to 1.36	1.0 to 1.36
Initial coolant Mach number	< 1.0	~ 1.0	0.187 to 1.168	0.29	0.48
Hot stream stagnation pressure, psia (N/cm ² abs)	520 to 2000 (289 to 1110)	~ 5000 (~ 2780)	~ 530 (~ 295)	3000 (1670)	3540 (1970)
Coolant stagnation temperature, $^{\circ}\text{R}$ (K)	540 to 870 (300 to 483)	517 to 563 (287 to 313)	417 to 655 (232 to 364)	~ 520 (~ 289)	~ 520 (~ 289)
Hot stream stagnation pressure, psia (N/cm ² abs)	~ 40 (~ 28)	500 (345)	~ 40 (~ 28)	~ 30 (~ 21)	~ 30 (~ 21)
Hot stream gas	Combustion products: JP-4 and air	Combustion products: JP-4 and oxygen	Air	Combustion products: JP-4 and air	Combustion products: JP-4 and air
Coolant	Air and helium	Nitrogen	Air and helium	Air	Air
External surface	Insulated	Insulated	Insulated	Noninsulated	Noninsulated

Power setting	Length, L,		Secondary diameter, D _s		Primary diameter, D _p	
	in.	cm	in.	cm	in.	cm
Maximum reheat	28.0	71.1	16.4	41.6	14.9	37.8
Reheat A	27.5	69.8	16.4	41.6	13.9	35.3

○ Thermocouple
 ● Wall static-pressure tap

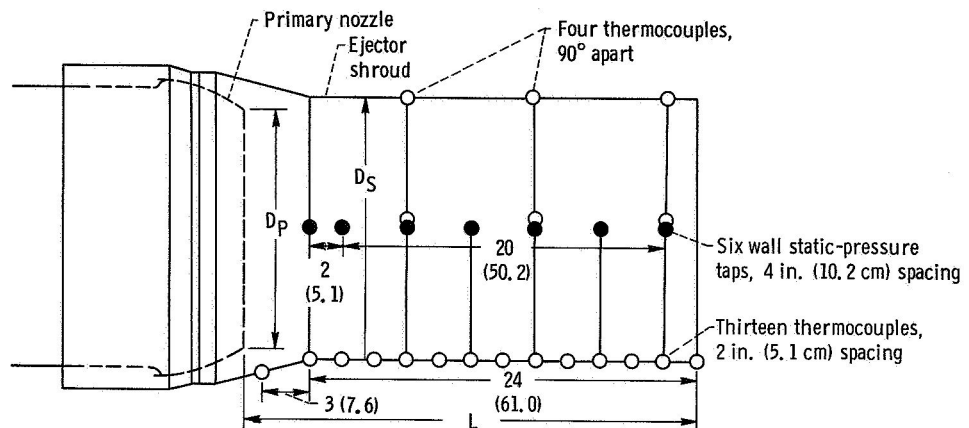


Figure 1. - Cylindrical ejector and instrumentation. (All dimensions are in inches (cm).)

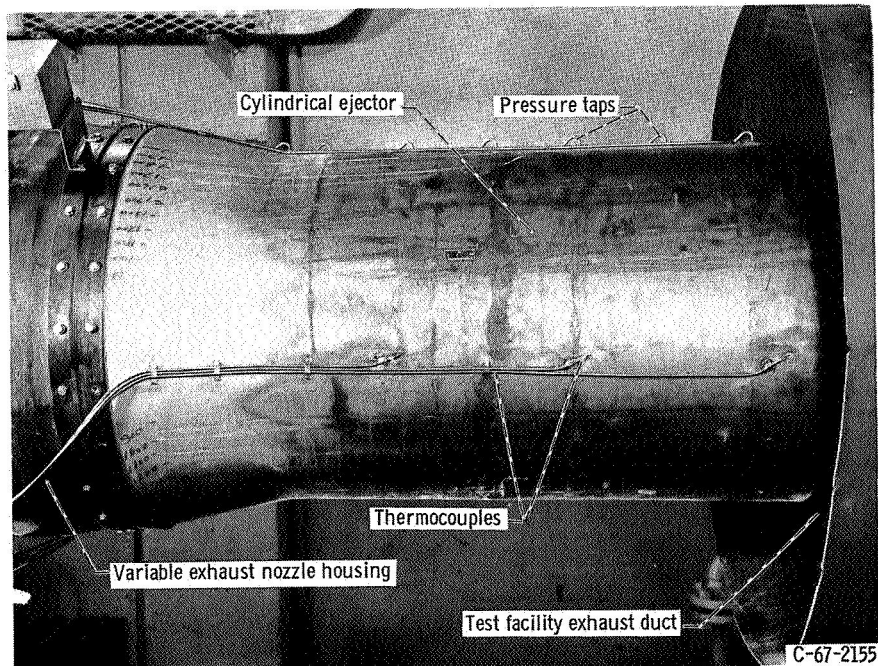


Figure 2. - Cylindrical ejector installed in facility.

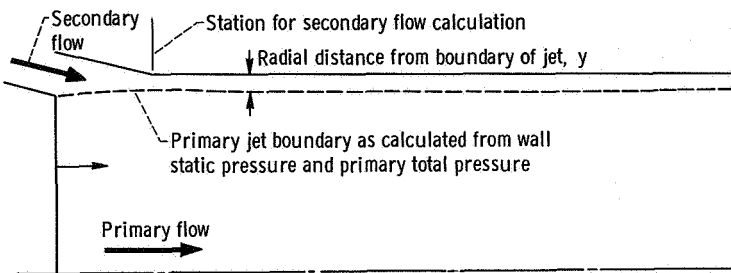


Figure 3. - Model used for calculation of secondary flow rate.

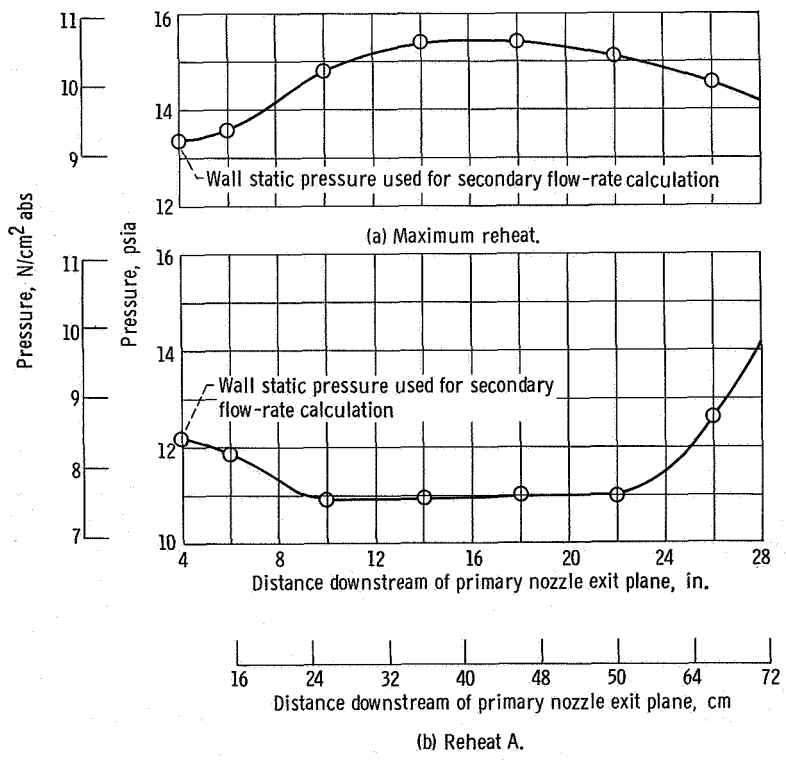
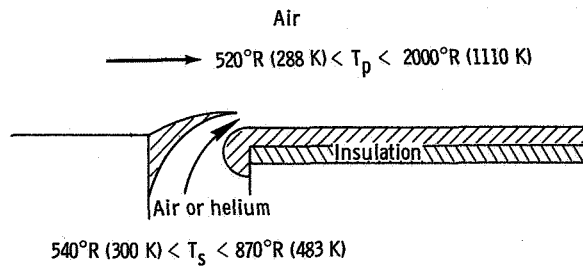
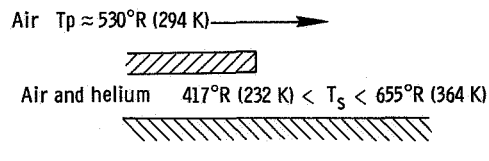
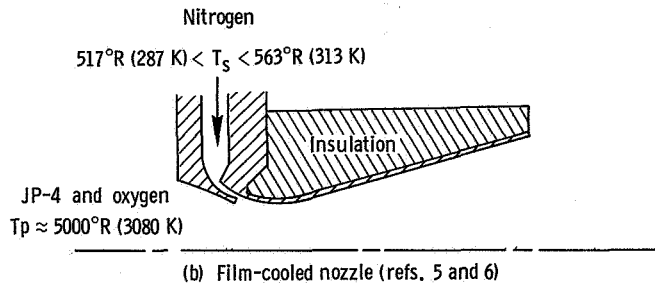


Figure 4. - Measured wall static pressure in ejector shroud.



(a) Flat plate coolant rig (refs. 2 to 4).



(c) Step-down slot (ref. 7).

Figure 5. - Various film-cooling schemes.

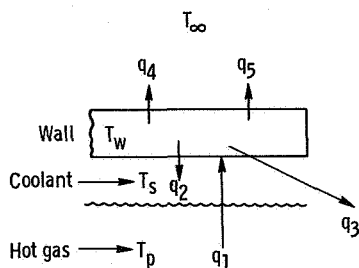


Figure 6. - Model used for correcting wall temperatures predicted by correlations.

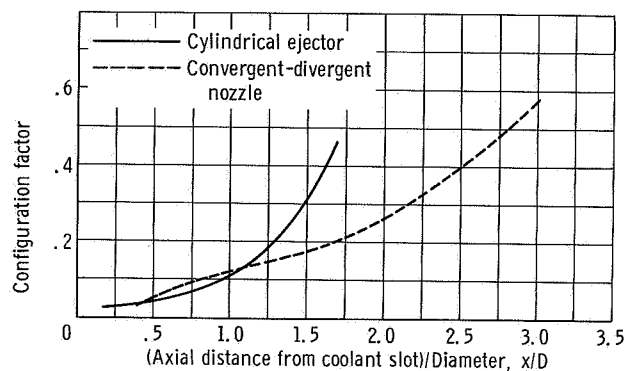
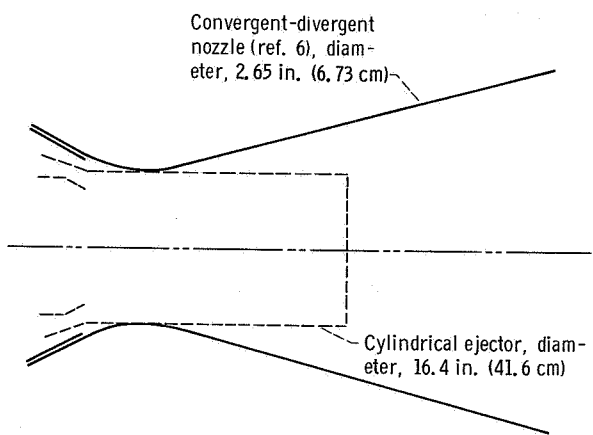


Figure 7. - Configuration factors for cylindrical ejector and convergent-divergent nozzle.

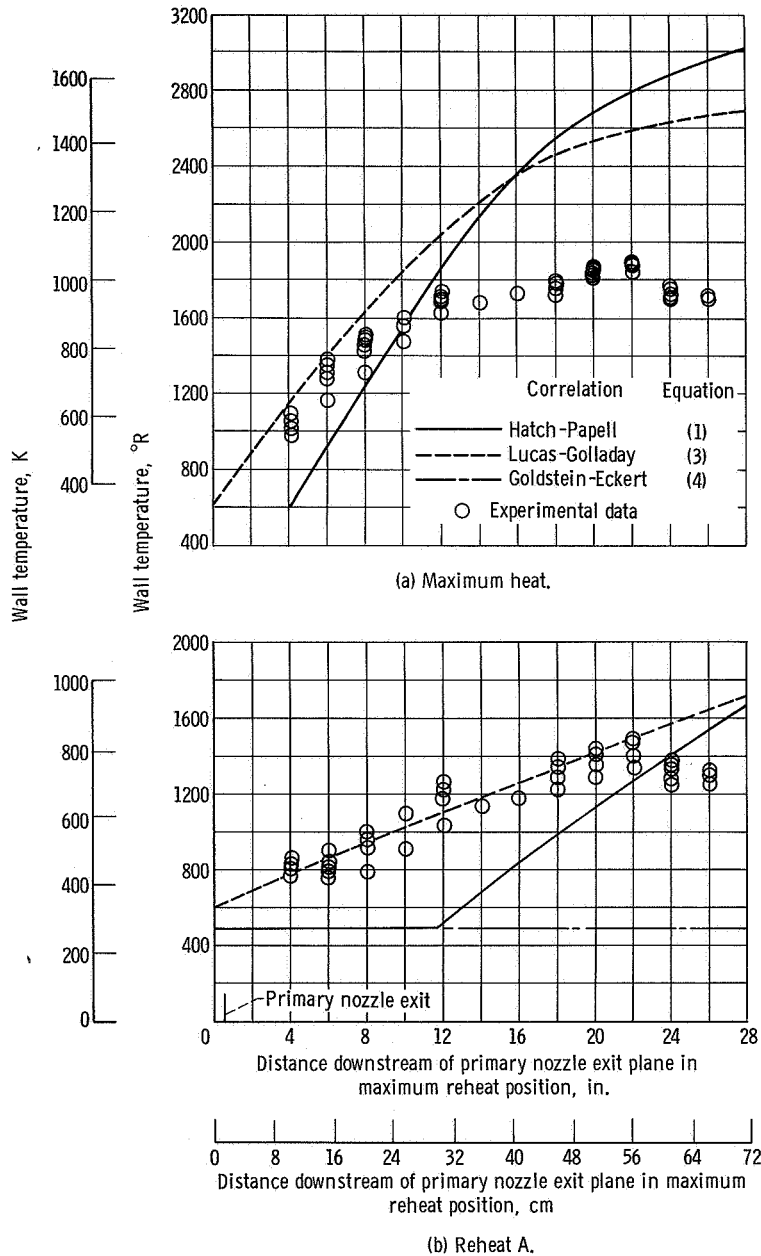


Figure 8. - Comparison of experimental and predicted temperature profiles.

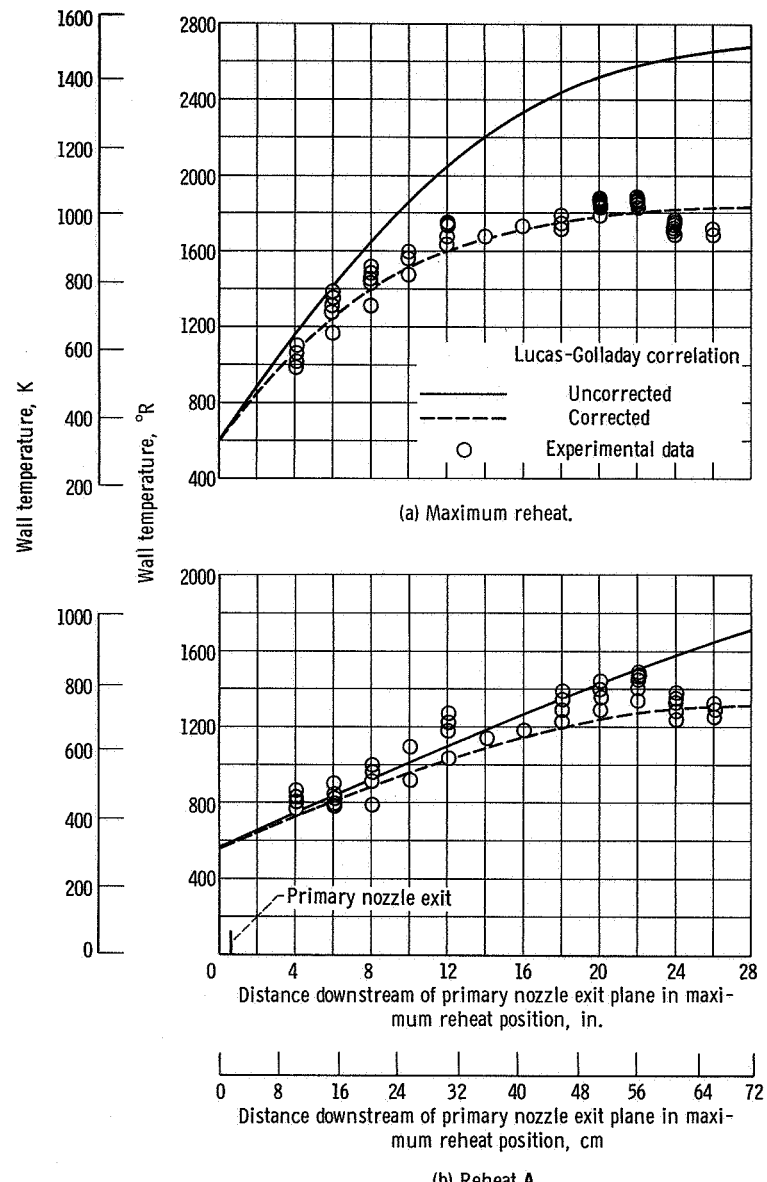


Figure 9. - Comparison of experimental data with corrected predictions using Lucas-Golladay correlation.

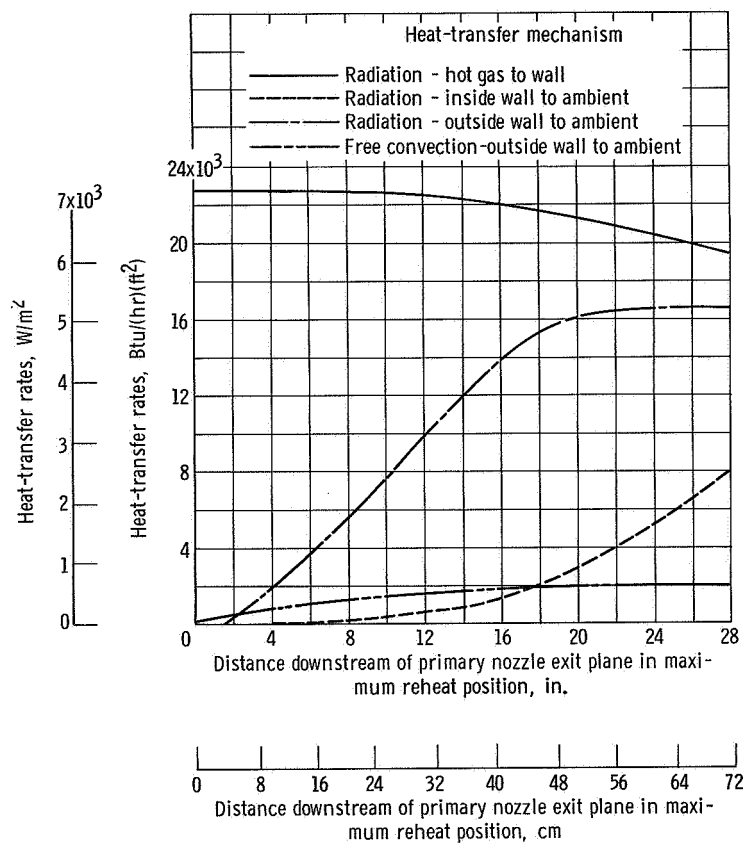


Figure 10. - Heat-transfer rates for maximum reheat engine power setting.

NATIONAL AERONAUTICS AND SPACE ADMINISTRATION
WASHINGTON, D.C. 20546
OFFICIAL BUSINESS

FIRST CLASS MAIL

POSTAGE AND FEES PAID
NATIONAL AERONAUTICS AND SPACE ADMINISTRATION

POSTMASTER: If Undeliverable (Section 1
Postal Manual) Do Not Re-

"The aeronautical and space activities of the United States shall be conducted so as to contribute . . . to the expansion of human knowledge of phenomena in the atmosphere and space. The Administration shall provide for the widest practicable and appropriate dissemination of information concerning its activities and the results thereof."

—NATIONAL AERONAUTICS AND SPACE ACT OF 1958

NASA SCIENTIFIC AND TECHNICAL PUBLICATIONS

TECHNICAL REPORTS: Scientific and technical information considered important, complete, and a lasting contribution to existing knowledge.

TECHNICAL NOTES: Information less broad in scope but nevertheless of importance as a contribution to existing knowledge.

TECHNICAL MEMORANDUMS: Information receiving limited distribution because of preliminary data, security classification, or other reasons.

CONTRACTOR REPORTS: Scientific and technical information generated under a NASA contract or grant and considered an important contribution to existing knowledge.

TECHNICAL TRANSLATIONS: Information published in a foreign language considered to merit NASA distribution in English.

SPECIAL PUBLICATIONS: Information derived from or of value to NASA activities. Publications include conference proceedings, monographs, data compilations, handbooks, sourcebooks, and special bibliographies.

TECHNOLOGY UTILIZATION PUBLICATIONS: Information on technology used by NASA that may be of particular interest in commercial and other non-aerospace applications. Publications include Tech Briefs, Technology Utilization Reports and Notes, and Technology Surveys.

Details on the availability of these publications may be obtained from:

SCIENTIFIC AND TECHNICAL INFORMATION DIVISION
NATIONAL AERONAUTICS AND SPACE ADMINISTRATION
Washington, D.C. 20546